
Article:
Hughes, P.J.C., Smith, L. orcid.org/0000-0002-5769-423X, Chan, H.-F. orcid.org/0000-0002-5382-2097 et al. (6 more authors) (2019) Assessment of the influence of lung inflation state on the quantitative parameters derived from hyperpolarized gas lung ventilation MRI in healthy volunteers. Journal of Applied Physiology, 126 (1). pp. 183-192. ISSN 8750-7587

https://doi.org/10.1152/japplphysiol.00464.2018

Title: Assessment of the influence of lung inflation state on the quantitative parameters derived from hyperpolarized gas lung ventilation MRI in healthy volunteers

Authors: Paul J.C. Hughes[1], Laurie Smith[1,2], Ho-Fung Chan[1], Bilal A. Tahir[1,3], Graham Norquay[1], Guilhem J. Collier[1], Alberto Biancardi[1,4], Helen Marshall[1] and Jim M. Wild[1]

[1]POLARIS, Academic Unit of Radiology, University of Sheffield, Sheffield, South Yorkshire, United Kingdom; [2]Sheffield Children's Hospital, Sheffield, UK; [3]Academic Unit of Clinical Oncology, University of Sheffield, Sheffield, South Yorkshire, UK; [4]Insigneo Institute for in silico Medicine, University of Sheffield, Sheffield, UK

Author contributions:

Paul J.C. Hughes: Conceived and designed research, performed experiments, analyzed data, interpreted results of experiments, prepared figures, drafted manuscript, edited and revised manuscript, approved final version of manuscript

Laurie Smith: Performed experiments, edited and revised manuscript, approved final version of manuscript

Bilal A. Tahir: Analyzed data, edited and revised manuscript, approved final version of manuscript

Ho-Fung Chan: Performed experiments, edited and revised manuscript, approved final version of manuscript

Graham Norquay: Performed experiments, edited and revised manuscript, approved final version of manuscript

Guilhem J. Collier: Performed experiments, edited and revised manuscript, approved final version of manuscript

Alberto Biancardi: edited and revised manuscript, approved final version of manuscript

Helen Marshall: Interpreted results of experiments, edited and revised manuscript, approved final version of manuscript

Jim M. Wild: Conceived and designed research, interpreted results of experiments, edited and revised manuscript, approved final version of manuscript

Corresponding Author: Professor Jim M. Wild, PhD, Academic Unit of Radiology, Department of Infection Immunity and Cardiovascular Disease, University of Sheffield; Floor C, Royal Hallamshire Hospital, S10 2JF; + 44 (0)114 2159141; j.m.wild@sheffield.ac.uk

Running head: Multiple lung inflation level imaging using HP gas MRI

ABSTRACT: In this study, the effect of lung volume on quantitative measures of lung ventilation was investigated using MRI with hyperpolarized ^{3}He and ^{129}Xe. Six volunteers were imaged with hyperpolarized ^{3}He at five different lung volumes (residual volume (RV), RV+1L, functional residual capacity (FRC), FRC+1L and total lung capacity (TLC)), and three were also imaged with hyperpolarized ^{129}Xe. Imaging at each of the lung volumes was repeated twice on the same day with corresponding ^{1}H lung anatomical images. Percentage lung ventilated volume (%VV) and variation of signal intensity (heterogeneity score, H_{score}) were evaluated. Increased ventilation heterogeneity, quantified by reduced %VV and increased H_{score}, was observed at lower lung volumes with the least ventilation heterogeneity observed at TLC. For ^{3}He MRI data, the coefficient of variation of %VV was less than 1.5% and less than 5.5% for H_{score} at all lung volumes, whilst for ^{129}Xe data the values were 4% and 10% respectively. Generally, %VV generated from ^{129}Xe images was lower than that seen from ^{3}He images. The good repeatability of ^{3}He %VV found here supports prior publications showing that percentage lung ventilated volume is a robust method for assessing global lung ventilation. The greater ventilation heterogeneity observed at lower lung volumes indicates that there may be partial airway closure in healthy lungs and that lung volume should be carefully considered for reliable longitudinal measurements of %VV and H_{score}. The results suggest that imaging patients at different lung volumes may help to elucidate obstructive disease pathophysiology and progression.

KEYWORDS: Imaging; MRI; Hyperpolarized gas; Lungs; Inflation;

NEW AND NOTEWORTHY: We present repeatability data of quantitative metrics of lung function derived from hyperpolarized helium-3, xenon-129 and proton anatomical images acquired at five lung volumes in volunteers. Increased regional ventilation heterogeneity at lower lung inflation levels was observed in the lungs of healthy volunteers.

ABSTRACT WORD COUNT: 246/250

NEW AND NOTEWORTHY WORD COUNT: 43/75

MANUSCRIPT WORD COUNT:

FIGURE COUNT: 9

TABLE COUNT: 7

Introduction

Hyperpolarized (HP) gas ventilation-weighed magnetic resonance imaging (MRI) allows the visualization of gas distribution within the lung and has been shown to detect early lung disease in patients with cystic fibrosis and normal spirometry (4, 19) and in the lungs of smokers (33). Additionally, it has been used to assess the response to treatment in patients with asthma (13, 29), to longitudinally assess patients with chronic obstructive pulmonary disease (17) and has been shown to be clinically feasible for assessing lung function in children (1).

HP gas and proton anatomical (^{1}H) lung magnetic resonance imaging (MRI) can be combined to quantify lung ventilation using percentage lung ventilated volume (%VV) or its counterpart the ventilation defect percentage (%VDP) (33), both of which have been widely adopted as simple and robust image-derived metrics. %VV is the ratio of the ventilated lung, defined from HP gas ventilation-weighted images to the thoracic cavity volume, defined from the ^{1}H anatomical images (16, 33). Previous work has shown improved repeatability of %VV when the anatomical image is acquired in the same breath-hold as the HP gas ventilation-weighted image (12).

Ventilation heterogeneity may be assessed by using the H_{score} metric developed by Tzeng et al. (31), which calculates the variation of signal intensity in a kernel around a given voxel as the standard deviation divided by the mean (e.g. Figure 1) (23, 31).

The clinical standard for assessing lung volumes is body plethysmography (22, 32), whilst changes in forced expiratory volume in one second (FEV_1) and forced vital capacity, measured using spirometry, are used as clinical markers for lung function

decline in certain diseases (22, 32). However, patient coaching of inhalation from a bag of gas rather than spirometric gating is generally used to achieve the lung volumes for HP gas MR imaging, which may lead to variability in lung volumes as will the ability of the patient to inhale the entire contents of the bag of gas being used. The most frequently used lung volume is functional residual capacity plus 1 liter (FRC+1L) (6-8, 16, 18, 27, 34). However, if a 1L bag is inhaled from FRC in smaller patients this volume may be close to total lung capacity (TLC) and thus understanding the effect of lung inflation level on these image-derived metrics is important.

Previous work by Muradyan et al. (23) analyzed the effect of inhalation of HP xenon-129 (^{129}Xe) from residual volume (RV) in healthy volunteers and sub-RV in elite divers by acquiring coronal projection images with an in-plane resolution of 4.7mm x 9.4mm. Muradyan et al. calculated the global H_{score} in the ventilated regions of the image, and found that when the elite divers inhaled low volumes of gas (0.9L and 0.4L respectively) compared to larger volumes of gas (1.3L and 0.9L respectively) from sub-RV, increased heterogeneity was seen in the images, consistent with punctate reopening of some airways that were closed at sub-RV. Marshall et al. (20) carried out preliminary work demonstrating the effect of airway opening between FRC+1L and TLC using HP ^{3}He imaging showing decreased heterogeneity and increased %VV at TLC when compared to FRC+1L. With these studies demonstrating important mechanisms at work in healthy controls and patients it is clear that understanding the effect of lung inflation on quantitative metrics derived from HP gas and ^{1}H anatomical MRI is an important step in moving these techniques forward into standard clinical practice.

Historically, noble gas MRI studies have made use of HP helium-3 (^{3}He); however, with the rising cost and scarcity of ^{3}He, the focus of the pulmonary imaging community is switching to the use of HP ^{129}Xe (18, 27) where differences in metrics have been reported due to the differences in diffusivity and the achievable signal of ^{129}Xe MRI. Thus the aims of this study were to use both HP ^{3}He and ^{129}Xe MRI to:

1. assess the effect of different lung inflation levels on the HP gas image derived metrics %VV and H_{score}.
2. assess the repeatability of %VV and H_{score} from two same-day imaging sessions.

Materials and methods

Subjects

The study was performed with national research ethics committee approval and with informed consent from all volunteers. Six volunteers (all male) were recruited for this study with the only criterion being that subjects were suitable for MRI and had no known respiratory complications. Two volunteers were former smokers, two were occasional smokers and two were never smokers. Table 1 shows the subject demographics.

Study protocol

Spirometry was performed to international standards (32) to ensure subjects had were defined as spirometrically free from respiratory conditions.

All ^{3}He imaging was carried out on a GE HDx 1.5T MRI scanner (GE Healthcare, Milwaukee, WI, USA) using a ^{3}He transmit-receive flexible chest coil (Clinical MR Solutions, Brookfield, WI, USA). ^{3}He was polarized using a commercial polarizer (GE Healthcare, Amersham, UK). HP ^{3}He 3D balanced steady state free precession and ^{1}H spoiled gradient echo images were acquired in the same breath (12) at five different lung volumes: RV, RV+1L, FRC, FRC+1L and TLC. For ^{129}Xe imaging, the gas was polarized using a home-built polarizer (24) and images were acquired using a ^{129}Xe transmit-receive flexible vest coil (Clinical MR Solutions, Brookfield, WI, USA) and the ^{1}H system body coil at five different lung volumes, as with ^{3}He imaging. ^{129}Xe and ^{1}H images were acquired in separate breath-holds as previously described (27, 28) and this was due to the longer acquisition time of the ^{129}Xe scan. Note that only a subset of the volunteers (V2, V3 and V6) were scanned using HP ^{129}Xe and separate-breath ^{1}H imaging as a feasibility study as some participants were no longer available to be scanned. A 1L mixture of hyperpolarized gas and nitrogen was used as it is the most commonly used volume in adults (6-8, 16, 18, 27, 34).

For the breathing maneuvers (Figure 2), volunteers were coached and instructed to breathe within the scanner by a pulmonary physiologist. During imaging, breathing maneuvers started with inhalation of the contents of the 1L bag from FRC, except for imaging at RV+1L where volunteers first exhaled to RV. To acquire images at TLC, volunteers inhaled room air to maximum lung capacity after the inhalation of 1L of gas from the bag. For imaging at FRC, volunteers inhaled the contents of the 1L bag from FRC and then exhaled back to FRC. For RV imaging, volunteers inhaled the contents of the 1L bag from FRC and then exhaled to RV. Gas doses were increased for the exhalation maneuvers and for imaging at TLC with the aim of ensuring

sufficient signal for imaging, and prior to exhalation participants held their breath for 5 seconds to allow the gas to diffuse into the peripheral lung. Inhaled gas doses are given in Table 2; note that images were also acquired in the order presented in Table 2.

For ^{3}He acquisitions, subjects were scanned twice on the same day, with a 10 to 20-minute break (remaining supine within the scanner) in between imaging sessions. ^{3}He imaging sessions lasted 20-30 minutes on average. For ^{129}Xe imaging, subjects were scanned twice on the same day, with a 20 to 40-minute break between imaging sessions and were removed from the scanner during this break. ^{129}Xe imaging sessions lasted 35-45 minutes on average, due to limitations imposed by gas polarization time.

Image analysis

Thoracic cavity volume (TCV) and ventilated volume (VV) were extracted from the ^{1}H anatomical and HP gas ventilation images, respectively, using the semi-automated segmentation method based on spatial Fuzzy C-means thresholding previously described (15). Percentage lung ventilated volume was calculated according to $\%VV = (VV/TCV) \times 100$.

Ventilation heterogeneity was assessed using a modified version of the H_{score} method previously described (31). Images were subsampled from 256x256 voxels in-plane to 128x128 voxels, resulting in an apparent image resolution of ~3.2x3.2x5mm for ^{3}He images or ~3.2x3.2x10mm for ^{129}Xe images. To avoid partial volume effects at the edge of the ventilation-weighted images, the TCV mask was eroded by 1 pixel, and

198 the ventilation-weighted image was then multiplied by the VV mask and eroded TCV
199 masks, with voxels outside of the VV and TCV masks being excluded from the local
200 heterogeneity calculation. To generate maps of ventilation heterogeneity, a 3x3 voxel
201 kernel (~9x9mm) was then passed over the images, centered on every voxel in the
202 ventilated volume, to calculate the local variation of signal intensity ($H_{i,j,k}$ at voxel
203 i,j,k). H_{score} in this work was then defined as the median of the non-zero values of the
204 local heterogeneity map rather than the mean as previously reported, as the
205 histograms of H_{score} were not normally distributed. For images acquired at TLC,
206 where there was clear signal dropout due to coil sensitivity coverage, VV and TCV
207 masks were matched, i.e. where signal dropout occurred emulating a defect it was
208 manually excluded on both the TCV and VV masks, in order to ensure that this did
209 not cause increased H_{score} and decreased %VV.
210
211 Additionally, the mean H_{score} of the most posterior slice was compared to the mean
212 H_{score} of the remaining image slices for each volunteer at each inflation level for the
213 data acquired with ^{3}He. The mean values were grouped by volunteer and lung volume
214 and significant differences were assessed using either a paired t-test or Wilcoxon
215 matched-pairs signed rank test depending on the normality of the data. This analysis
216 was not carried out for ^{129}Xe data due to the reduced number of subjects.
217
218 *Repeatability and statistical analysis*
219 To assess the repeatability of %VV and H_{score} between session 1 (S1) and session 2
220 (S2), the coefficient of variation (CoV), Bland-Altman analysis (2), paired t-tests and
221 the repeatability limit were used. For CoV analysis, values were grouped by inflation
222 level and session e.g. RV S1 for all volunteers was compared to RV S2 for all

volunteers. Additionally, to assess repeatability in the image domain voxel-wise correlation (25) was carried out where each of the six same-inflation inter-session image pairs were spatially aligned via deformable image registration (3), in order to facilitate computation of Spearman correlation coefficients as previously described (30). The repeatability limit was calculated as $1.96 \times \sqrt{2}s_w$, where s_w is the within-subjects standard deviation calculated using SPSS (version 23, IBM) (21).

Spearman's correlation was also used to assess the relationship between TCV and %VV and H_{score} along with the relationship between TCV and the absolute change of %VV and H_{score} over the two imaging sessions. Finally, a two-way repeated measures analysis of variance was performed to statistically validate the effect of lung volume on H_{score} and %VV where within subject factors were defined as the imaging session and lung inflation level, and multiple comparisons were carried out using the Tukey correction. Voxel-wise correlation and two-way repeated measures analysis of variance was not carried out for the ^{129}Xe data due to the reduced number of subjects scanned.

Results

Comparison of HP ^{129}Xe and HP ^{3}He MRI at different inflation levels

The SNR of the ^{129}Xe images was lower than the SNR of the ^{3}He images, particularly at RV, RV+1L and FRC, as can be seen in Figure 3. The RV image of HV3 (^{129}Xe, session 2) had complete loss of signal from posterior sections of the lung due to a coil sensitivity issue at the time of the experiment and was thus excluded from analysis. ^{129}Xe images had consistently lower %VV ($p<0.0001$) and higher H_{score} ($p<0.0001$) when compared to those obtained with HP ^{3}He (Tables 3 and 4).

The effect of lung inflation level on %VV and H_{score}

The effect of lung inflation level on ^{3}He and ^{129}Xe images acquired at different lung volumes is shown in Figure 4 for volunteer 2. There was a trend towards increased ventilation homogeneity at higher lung volumes, which was seen using both gases. For ^{3}He data significant differences between H_{score} were found when comparing TLC to all other lung volumes via the two-way analysis of variance ($p<0.0001$ for all). No other significant differences in H_{score} between different inflation levels were found.

%VV also varied with lung volume as can be seen from the mean values of %VV and H_{score} shown in Table 4 which are visualized in Figure 5. For ^{3}He data, %VV at RV and FRC+1L were the only volumes that were significantly different from each other when compared using the two-way analysis of variance ($p=0.0155$). Lung volume had a significant effect on both %VV ($p=0.0265$) and H_{score} ($p<0.0001$).

When considering the ^{1}H MRI acquired in the same breath as ^{3}He MRI, TCV generated from the ^{1}H images correlated strongly with H_{score} ($r=-0.75$, $p<0.0001$) but not with %VV ($r=0.27$, $p=0.15$). TCV had a weak correlation with the absolute change in %VV ($r=-0.39$, $p=0.03$) but not H_{score} ($r=0.01$, $p=0.53$). For the ^{1}H MRI acquired in a separate breath to the ^{129}Xe MRI, TCV had a strong correlation with H_{score} ($r=-0.90$, $p<0.0001$) and a moderate correlation with the absolute change of H_{score} over the two sessions ($r=-0.66$, $p=0.01$). TCV had no significant correlation with %VV or the absolute change in %VV over both sessions ($r=0.44$, $p=0.12$ and $r=-0.33$, $p=0.25$ respectively).

Regardless of the acquisition volume increased H_{score} was seen in the posterior region of the lung (Figure 6) with the most posterior slice having a mean±SD H_{score} over all volunteers and inflation levels of 15.4±7.1% whilst all other slices combined had values of 9.8±3.1% when considering ^{3}He data. Additionally, significant differences between the most posterior slice and the remaining slices (Table 5) of the image were seen at RV+1L and FRC+1L (p=0.0087 and p=0.031 respectively) whilst no significant difference was seen at RV, FRC and TLC (p = 0.1562, p=0.3125 and p=0.0790 respectively).

Repeatability of %VV and H_{score}

Table 6 shows the CoV of %VV and H_{score} over all 6 volunteers at each of the lung volumes imaged with ^{3}He and over all 3 volunteers imaged with ^{129}Xe. For ^{3}He data, CoV was less than 1.5% for %VV and less than 5.5% for H_{score} at all lung volumes. Concerning ^{129}Xe data, CoV was less than 4% for %VV and less than 10% for H_{score} at all lung volumes.

Concerning the ^{3}He data, strong inter-session voxel-wise correlation was observed for all lung volumes (mean±SD Spearman coefficients: 0.92±0.03 for RV; 0.94±0.03 for RV+1L; 0.95±0.02 for FRC; 0.95±0.03 for FRC+1L; 0.93±0.02 for TLC).

Bland-Altman bias±limits of agreement (LOA) are visualized in Figures 7 (^{3}He) and 8 (^{129}Xe) for both %VV (A) and H_{score} (B). For ^{3}He data, the limits of agreement were less than 5% for %VV, and less than 2.5% for H_{score}. For ^{129}Xe data, the limits of agreement were less than 10% for %VV, and less than 4% for H_{score}. For ^{3}He MRI the bias for %VV was less than 2% at all lung volumes whilst H_{score} bias was less than

1% at all lung volumes whilst for ^{129}Xe MRI %VV bias was less than 6% at all lung volumes and H_{score} bias was less than 2% at all lung volumes.

Table 7 details the repeatability limit for %VV and H_{score} from both HP ^{3}He and ^{129}Xe images. When considering ^{3}He data %VV repeatability was less than 3% for all volumes except RV and less than 2% for all volumes when considering H_{score}. When considering ^{129}Xe data %VV repeatability was less than 10% for all volumes except RV and less than 3% for all volumes when considering H_{score}.

Discussion

The work carried out here has demonstrated that lung volume has a significant bearing on quantitative measurements of lung ventilation derived from both ^{3}He and ^{129}Xe MRI. Additionally, from the effect of lung volume on the quantitative metrics of %VV and H_{score} evident in healthy volunteers, it can be concluded that the lung volume during imaging must be well controlled to ensure that these metrics can be used reliably in longitudinal studies.

Imaging over all volunteers revealed increased ventilation heterogeneity at lower lung volumes, potentially indicating partial airway closure in certain regions of the lung. Increased heterogeneity was particularly observed in the posterior section of the lung at RV+1L, exemplified by the median H_{score} per slice plotted against slice number for V5 in Figure 9. This increased heterogeneity is likely due to the breathing maneuver used to obtain the images at RV+1L, that is the volunteers first exhaled to RV, which may have caused some airway closure. In contrast, the HP gas mixture was inhaled from FRC for all other lung volumes, and so the ventilation seen in the RV and FRC

images was influenced by the gas distribution within the lungs at FRC+1L. Note that although increased heterogeneity is seen in the anterior portion of the lung, the increased H_{score} in those areas are due to the reduced SNR due to decreased gas reaching those areas within the lung.

This increased ventilation heterogeneity at RV+1L in volunteers suggests the same underpinning mechanisms as reported in the work by Muradyan et al. (23), where there were distinct focal areas of lung affected by airway closure after inhalation of small gas volumes from below residual volume in elite divers. We hypothesize that the areas of decreased ventilation signal at RV+1L were caused by airways remaining closed following inhalation of the gas mixture. We believe that this same effect was not observed at RV in the current study since the maneuver to RV required first inhaling to FRC+1L, such that gas would remain in the areas opened by this first inhalation maneuver even if the airways were to close later on. The areas of reduced ventilation in lungs of the elite divers following inhalation from sub-RV levels observed in the work by Muradyan et al. (23) were larger than those seen here in these volunteers, whilst they did not see the same heterogeneity seen here in their volunteers following inhalation from RV. One possible reason for this is the improvements in the image resolution for ^{129}Xe when compared to their experiments that were carried out with 2D projection imaging, and thus providing us with better spatial sampling of regional heterogeneity.

Imaging after smaller inspirations from RV would be interesting in order to assess at which point the ventilation heterogeneity would return to a distribution closer to that seen at FRC or FRC+1L. In this case, it would be expected that the smaller the

volume inhaled from RV, the greater the ventilation heterogeneity would be; although the feasibility of these experiments would be limited by the volume of HP gas required for sufficient image SNR if carrying the experiment out with ^{129}Xe. Another factor which may contribute to increased H_{score} at RV when compared to FRC+1L and FRC is the increased ratio of blood vessel volume to lung volume at RV, resulting in increased H_{score}.

The small CoV of %VV between sessions further confirms the growing body of evidence that %VV is a robust global metric of lung ventilation (5, 12, 17) , and the high inter-scan repeatability makes %VV (or VDP) a good candidate metric for longitudinal assessment of lung function in patients (17). The proportionally larger CoV of the H_{score} suggests that this measure of global ventilation image heterogeneity may be less repeatable.

The generally lower SNR of ^{129}Xe images when compared to ^{3}He images is a well-known phenomenon and follows previous publications (14, 28), with ^{129}Xe acquisitions having a mean±SD SNR of 30±13 compared to the 42±15 of the ^{3}He acquisitions. Consequently, the higher H_{score} seen in the ^{129}Xe images when compared to images acquired with HP ^{3}He is at least partially due to the lower SNR and thus increased heterogeneity of signal within ventilated regions. The lower %VV values measured from ^{129}Xe images compared to ^{3}He images may be due to the lower diffusivity of ^{129}Xe compared to ^{3}He, and are consistent with %VV values reported previously in healthy volunteers, patients with chronic obstructive pulmonary disease and patients with lung cancer who were imaged with both gases (18, 27). Furthermore, lower SNR in one of the ^{129}Xe acquisitions (V6, RV, S1) caused an increase in H_{score}

showing that the maneuvers or gas doses need to be optimized for the ^{129}Xe imaging acquisitions if this methodology is applied to patient cohorts. The need to register the anatomical images to the ventilation images for ^{129}Xe %VV calculation will also contribute to the lower repeatability of ^{129}Xe %VV when compared to ^{3}He %VV (12), where anatomical images were acquired in the same breath-hold. Additionally, due to imaging constraints, HP ^{129}Xe images were acquired with double the slice thickness (10mm) of the HP ^{3}He images (5mm); thus, differences would be expected due to different inherent physical properties and image acquisition considerations of the respective gas.

Imaging patients with HP gas at different lung volumes may provide a clearer picture of the nature of lung disease. For example, in patients with obstructive lung disease, following deep inhalation to TLC, the effect of increased positive pressure within the airways may result in a reduced H_{score} and increased %VV due to opening of obstructed airways (20). Additionally, as patients with chronic respiratory disease may have increased closing volumes, imaging at expiration may identify areas of gas trapping similar to those observed by Holmes et al. (9-11).

An increased number of healthy volunteers with a larger age range, and inclusion of female subjects would extend this preliminary work into the effect of lung volume on ventilation heterogeneity in healthy volunteers. Additionally, mitigating the signal dropout seen in TLC images with larger coil coverage is an important consideration for future studies. The smoking history of four of the six volunteers (two former smokers and two occasional smokers) means that these data may not represent the ventilation patterns seen in a group of healthy never-smokers. However, the number

of pack years reported by the volunteers scanned was low (<0.7), and in a previous ^{3}He MRI study of pulmonary ventilation (26) three of the smokers would have been classified as never-smokers (<0.5 pack years). However, the volunteers scanned were spirometrically defined as free from respiratory disease and not unrepresentative of the general population in terms of smoking history. The fact that increased ventilation heterogeneity at lower lung inflation levels was seen in the two never smokers as well as those with a smoking history suggests this effect is not due to smoking related obstructive airways disease.

Conclusions

Increased ventilation heterogeneity was observed in HP gas images acquired at lower lung volumes in healthy volunteers. This work has shown that although TLV and VV may vary considerably between repeated scans there was little effect on %VV in these healthy volunteers. This indicates it may be important to image patients over a range of lung volumes with different breathing maneuvers to fully understand disease progression and accurately characterize ventilation defects and pulmonary mechanics. Finally, the variation in lung volume must be considered when monitoring patients longitudinally with hyperpolarized gas MRI particularly in the cases of disease with a reversible nature such as asthma.

Acknowledgements: The authors thank Mr. Oliver Rodgers for aiding with the scanning of volunteers.

Grants: The authors thank the University of Sheffield, the HEE/NIHR (NIHR-RP-R3-12-027, ICA-CDRF-2015-01-027), Sheffield Hospitals Charity (161731) and the MRC (MR/M008894/1) for funding this research.

Disclosures: Paul J.C. Hughes – PhD part-funded by GlaxoSmithKline (STU100037614).

References

1. **Altes TA, Meyer CH, Mata JF, Froh DK, Paget-Brown A, Teague WG, Fain SB, de Lange EE, Ruppert K, and Botfield MC**. Hyperpolarized helium-3 magnetic resonance lung imaging of non-sedated infants and young children: a proof-of-concept study. *Clinical imaging* 45: 105-110, 2017.
2. **Altman DG, and Bland JM**. Measurement in medicine: the analysis of method comparison studies. *The statistician* 307-317, 1983.
3. **Avants BB, Tustison NJ, Song G, Cook PA, Klein A, and Gee JC**. A reproducible evaluation of ANTs similarity metric performance in brain image registration. *NeuroImage* 54: 2033-2044, 2011.
4. **Bannier E, Cieslar K, Mosbah K, Aubert F, Duboeuf F, Salhi Z, Gaillard S, Berthezène Y, Crémillieux Y, and Reix P**. Hyperpolarized 3He MR for sensitive imaging of ventilation function and treatment efficiency in young cystic fibrosis patients with normal lung function. *Radiology* 255: 225-232, 2010.
5. **Fain SB, Korosec FR, Holmes JH, O'Halloran R, Sorkness RL, and Grist TM**. Functional lung imaging using hyperpolarized gas MRI. *Journal of Magnetic Resonance Imaging* 25: 910-923, 2007.
6. **Guo F, Yuan J, Rajchl M, Svenningsen S, Capaldi DP, Sheikh K, Fenster A, and Parraga G**. Globally optimal co-segmentation of three-dimensional pulmonary 1 H and hyperpolarized 3 He MRI with spatial consistence prior. *Medical image analysis* 23: 43-55, 2015.
7. **He M, Driehuys B, Que LG, and Huang Y-CT**. Using hyperpolarized 129Xe MRI to quantify the pulmonary ventilation distribution. *Academic radiology* 23: 1521-1531, 2016.
8. **Heydarian M, Kirby M, Wheatley A, Fenster A, and Parraga G**. Two and three-dimensional segmentation of hyperpolarized 3 He magnetic resonance imaging of pulmonary gas distribution. In: *Medical Imaging 2012: Biomedical Applications in Molecular, Structural, and Functional Imaging*International Society for Optics and Photonics, 2012, p. 83171C.
9. **Holmes JH, Korosec FR, Du J, O'halloran RL, Sorkness RL, Grist TM, Kuhlman JE, and Fain SB**. Imaging of lung ventilation and respiratory dynamics in a single ventilation cycle using hyperpolarized He- 3 MRI. *Journal of Magnetic Resonance Imaging* 26: 630-636, 2007.
10. **Holmes JH, O'halloran RL, Brodsky EK, Bley TA, Francois CJ, Velikina JV, Sorkness RL, Busse WW, and Fain SB**. Three- dimensional imaging of ventilation dynamics in asthmatics using multiecho projection acquisition with constrained reconstruction. *Magnetic resonance in medicine* 62: 1543-1556, 2009.
11. **Holmes JH, O'Halloran RL, Brodsky EK, Jung Y, Block WF, and Fain SB**. 3D hyperpolarized He- 3 MRI of ventilation using a multi- echo projection acquisition. *Magnetic resonance in medicine* 59: 1062-1071, 2008.
12. **Horn F, Tahir B, Stewart N, Collier G, Norquay G, Leung G, Ireland R, Parra- Robles J, Marshall H, and Wild J**. Lung ventilation volumetry with same-breath acquisition of hyperpolarized gas and proton MRI. *NMR in biomedicine* 27: 1461-1467, 2014.
13. **Horn FC, Marshall H, Collier GJ, Kay R, Siddiqui S, Brightling CE, Parra-Robles J, and Wild JM**. Regional Ventilation Changes in the Lung: Treatment Response Mapping by Using Hyperpolarized Gas MR Imaging as a Quantitative Biomarker. *Radiology* 284: 854-861, 2017.

14. **Horn FC, Rao M, Stewart NJ, and Wild JM**. Multiple breath washout of hyperpolarized 129Xe and 3He in human lungs with three- dimensional balanced steady- state free- precession imaging. *Magnetic resonance in medicine* 77: 2288-2295, 2017.
15. **Hughes PJ, Horn FC, Collier GJ, Biancardi A, Marshall H, and Wild JM**. Spatial fuzzy c- means thresholding for semiautomated calculation of percentage lung ventilated volume from hyperpolarized gas and 1H MRI. *Journal of Magnetic Resonance Imaging* 47: 640-646, 2018.
16. **Kirby M, Heydarian M, Svenningsen S, Wheatley A, McCormack DG, Etemad-Rezai R, and Parraga G**. Hyperpolarized 3He Magnetic Resonance Functional Imaging Semiautomated Segmentation. *Academic radiology* 19: 141-152, 2012.
17. **Kirby M, Mathew L, Wheatley A, Santyr GE, McCormack DG, and Parraga G**. Chronic obstructive pulmonary disease: longitudinal hyperpolarized 3He MR imaging. *Radiology* 256: 280-289, 2010.
18. **Kirby M, Svenningsen S, Owrangi A, Wheatley A, Farag A, Ouriadov A, Santyr GE, Etemad-Rezai R, Coxson HO, and McCormack DG**. Hyperpolarized 3He and 129Xe MR imaging in healthy volunteers and patients with chronic obstructive pulmonary disease. *Radiology* 265: 600-610, 2012.
19. **Marshall H, Horsley A, Taylor CJ, Smith L, Hughes D, Horn FC, Swift AJ, Parra-Robles J, Hughes PJ, and Norquay G**. Detection of early subclinical lung disease in children with cystic fibrosis by lung ventilation imaging with hyperpolarised gas MRI. *Thorax* 72: 760-762, 2017.
20. **Marshall H, Siddiqui S, Leung G, Parra-Robles J, Xu X, Brightling C, and Wild J**. Imaging The Effect Of Airway Opening In Asthma Due To Inflation State With 3He MRI. In: *B109 TECHNOLOGIC ADVANCES IN IMAGING FOR PHENOTYPING LUNG DISEASE*Am Thoracic Soc, 2013, p. A3744-A3744.
21. **McAlinden C, Khadka J, and Pesudovs K**. Precision (repeatability and reproducibility) studies and sample-size calculation. *Journal of Cataract & Refractive Surgery* 41: 2598-2604, 2015.
22. **Miller MR, Hankinson J, Brusasco V, Burgos F, Casaburi R, Coates A, Crapo R, Enright Pv, Van Der Grinten C, and Gustafsson P**. Standardisation of spirometry. *European respiratory journal* 26: 319-338, 2005.
23. **Muradyan I, Loring SH, Ferrigno M, Lindholm P, Topulos GP, Patz S, and Butler JP**. Inhalation heterogeneity from subresidual volumes in elite divers. *Journal of Applied Physiology* 109: 1969-1973, 2010.
24. **Norquay G, Parnell SR, Xu X, Parra-Robles J, and Wild JM**. Optimized production of hyperpolarized 129Xe at 2 bars for in vivo lung magnetic resonance imaging. *Journal of Applied Physics* 113: 044908, 2013.
25. **Reinstein DZ, Archer TJ, Silverman RH, and Coleman DJ**. Accuracy, repeatability, and reproducibility of Artemis very high-frequency digital ultrasound arc-scan lateral dimension measurements. *Journal of Cataract & Refractive Surgery* 32: 1799-1802, 2006.
26. **Sheikh K, Paulin GA, Svenningsen S, Kirby M, Paterson NA, McCormack DG, and Parraga G**. Pulmonary ventilation defects in older never-smokers. *Journal of applied physiology* 117: 297-306, 2014.
27. **Stewart N, Chan H-F, Hughes PJC, Horn FC, Norquay G, Rao M, Yates DP, Ireland RH, Hatton MQ, Tahir BA, Ford P, Swift AJ, Lawson R, Marshall H, Collier GJ, and Wild JM**. Comparison of 3He and 129Xe MRI for evaluation of

lung microstructure and ventilation at 1.5 T. Journal of Magnetic Resonance Imaging, 2018.

28. **Stewart NJ, Norquay G, Griffiths PD, and Wild JM**. Feasibility of human lung ventilation imaging using highly polarized naturally abundant xenon and optimized three- dimensional steady- state free precession. *Magnetic resonance in medicine* 74: 346-352, 2015.

29. **Svenningsen S, Kirby M, Starr D, Leary D, Wheatley A, Maksym GN, McCormack DG, and Parraga G**. Hyperpolarized 3He and 129Xe MRI: differences in asthma before bronchodilation. *Journal of Magnetic Resonance Imaging* 38: 1521-1530, 2013.

30. **Tahir B, Hughes P, Robinson S, Marshall H, Stewart N, Norquay G, Biancardi A, Chan H-F, Collier G, and Hart K**. Spatial comparison of CT-based surrogates of lung ventilation with hyperpolarized Helium-3 and Xenon-129 gas MRI in patients undergoing radiation therapy. *International Journal of Radiation Oncology• Biology• Physics* 2018.

31. **Tzeng Y-S, Lutchen K, and Albert M**. The difference in ventilation heterogeneity between asthmatic and healthy subjects quantified using hyperpolarized 3He MRI. *Journal of Applied Physiology* 106: 813-822, 2009.

32. **Wanger J, Clausen J, Coates A, Pedersen O, Brusasco V, Burgos F, Casaburi R, Crapo R, Enright P, and Van Der Grinten C**. Standardisation of the measurement of lung volumes. *European Respiratory Journal* 26: 511-522, 2005.

33. **Woodhouse N, Wild JM, Paley MN, Fichele S, Said Z, Swift AJ, and van Beek EJ**. Combined helium- 3/proton magnetic resonance imaging measurement of ventilated lung volumes in smokers compared to never- smokers. *Journal of magnetic resonance imaging* 21: 365-369, 2005.

34. **Zha W, Niles DJ, Kruger SJ, Dardzinski BJ, Cadman RV, Mummy DG, Nagle SK, and Fain SB**. Semiautomated ventilation defect quantification in exercise-induced bronchoconstriction using hyperpolarized helium-3 magnetic resonance imaging: a repeatability study. *Academic radiology* 23: 1104-1114, 2016.

555 **FIGURE LEGENDS**

556 **Figure 1** Example of local H_{score} calculation in the RV+1L ventilation-weighted
557 image of volunteer 5 (top image). The yellow box on the left shows an area of low
558 H_{score} (enhanced image on the left, with the local area outlined and the voxel that is
559 replaced denoted with an 'x'), which is highlighted with the blue box in the H_{score} map
560 (lower image). The same is shown for a region of high H_{score} on the right.

561 **Figure 2** Breathing maneuvers and acquisition volumes used in this study. Solid gray
562 lines indicate an inhalation from a 1L bag, solid black lines indicate an exhalation and
563 dashed gray lines indicate an inhalation of room air. Solid boxes represent acquisition
564 volumes and dashed boxes represent intermediate volumes as part of the breathing
565 maneuver.

566 **Figure 3** Signal-to-noise ratio (SNR) values from the volunteers scanned with both
567 ^{3}He and ^{129}Xe only.

568 **Figure 4** Representative slices from all acquisition volumes in V2 from both ^{3}He and
569 ^{129}Xe images. The top row shows the ^{3}He images and the bottom row the ^{129}Xe
570 images acquired in V2.

571 **Figure 5** Plots of (A) percentage lung ventilated volume from ^{3}He data, (B) H_{score} (%)
572 from ^{3}He data, (C) percentage lung ventilated volume from ^{129}Xe data and (D) H_{score}
573 (%) from ^{129}Xe data at each acquisition volume. Each circle represents a volunteer
574 whilst the lines represent the mean of the values.

575 **Figure 6** Representative posterior slices of HP ^{3}He ventilation images and
576 heterogeneity maps at all acquisition volumes from V2. The arrows are pointing to
577 areas of decreased ventilation and increased H_{score}.

578 **Figure 7** Bland-Altman plots of (A) %VV and (B) H_{score} generated from images
579 acquired with HP ^{3}He at all acquisition volumes. Black dots indicate bias, gray dots
580 are the 95% confidence intervals and the black dashed line is 0.
581 **Figure 8** Bland-Altman plots of (A) %VV and (B) H_{score} generated from images
582 acquired with HP ^{129}Xe at all acquisition volumes. Black dots indicate bias, gray dots
583 are the 95% confidence intervals and the black dashed line is 0.
584 **Figure 9** Exemplary plot of H_{score} from anterior to posterior for V5.
585

Table 1 Subject demographics. V = volunteer, FEV_1 = Forced expiratory volume in 1 second % predicted

Subject	Age, yr	Height, cm	Weight, kg	FEV_1	Pack years
V1	32	183.0	87.0	102.0	0.15
V2	35	184.0	76.0	77.2	0.13
V3	31	182.0	83.0	105.0	0.06
V4	34	185.6	94.0	83.6	0.70
V5	27	189.5	74.0	102.9	0
V6	28	187.6	90.0	99.9	0

Table 2 Gas doses for hyperpolarized (HP) helium-3 (^{3}He) and xenon-129 (^{129}Xe) acquisitions reported as HP gas dose (N_2), where N_2 = nitrogen. RV = residual volume, RV+1L = residual volume plus 1 liter of gas mixture, FRC = functional residual capacity, FRC+1L = functional residual capacity volume plus 1 liter of gas mixture and TLC = total lung capacity

Acquisition	**^{3}He (N_2), ml**	**^{129}Xe (N_2), ml**
RV	200 (800)	1000 (0)
RV+1L	150 (850)	750 (250)
FRC	200 (800)	1000 (0)
FRC+1L	150 (850)	600 (400)
TLC	200 (800)	750 (250)

Table 3 Mean percentage lung ventilated volume (%VV) and median score of the heterogeneity map (H_{score}) values at each lung volume and session (session 1 (S1)/session 2 (S2)) over all volunteers derived from hyperpolarized helium-3 (^{3}He) and xenon-129 (^{129}Xe)

	RV S1	**RV S2**	**RV+1L S1**	**RV+1L S2**	**FRC S1**	**FRC S2**	**FRC+1L S1**	**FRC+1L S2**	**TLC S1**	**TLC S2**
%VV ^{3}He	95.65	97.17	97.39	97.84	97.30	97.80	98.18	98.05	97.33	97.98
H_{score} ^{3}He	10.47	9.98	10.12	10.1	9.37	9.23	9.10	9.20	7.55	7.39
%VV ^{129}Xe	82.94	87.43	92.36	90.86	93.53	94.99	92.99	96.55	95.83	94.98
H_{score} ^{129}Xe	15.89	14.92	11.51	12.29	10.83	10.99	11.09	10.53	8.71	8.24

Table 4 Average percentage lung ventilated volume (%VV) and median score of the heterogeneity map (H_{score}) values over session 1 and session 2 generated from hyperpolarized helium-3 (^{3}He) and xenon-129 (^{129}Xe) images for the three volunteers (V) scanned with both gases

Acquisition	**%VV ^{3}He V2**	**%VV ^{129}Xe V2**	**%VV ^{3}He V3**	**%VV ^{129}Xe V3**	**%VV ^{3}He V6**	**%VV ^{129}Xe V6**
RV	98.68	96.26	97.03	**NA**	95.41	88.88
RV+1L	97.67	90.46	99.49	91.54	98.26	92.84
FRC	98.85	97.53	98.34	94.41	97.85	90.85
FRC+1L	98.46	96.70	98.76	94.51	98.10	93.11
TLC	99.46	95.58	99.12	93.14	97.82	97.50
Acquisition	**H_{score} ^{3}He V2**	**H_{score} ^{129}Xe V2**	**H_{score} ^{3}He V3**	**H_{score} ^{129}Xe V3**	**H_{score} ^{3}He V6**	**H_{score} ^{129}Xe V6**
RV	8.96	12.53	11.63	**NA**	10.16	16.16
RV+1L	10.26	12.08	8.82	11.74	9.04	11.89
FRC	8.85	11.01	9.15	10.91	8.90	10.82
FRC+1L	9.33	10.83	8.61	10.62	8.59	10.98
TLC	6.15	8.10	7.33	8.95	6.50	8.38

Table 5 Mean H_{score} (over session 1 and session 2) at the most posterior slice and all remaining slices for all volunteers at each lung volume for all images acquired using hyperpolarized helium-3

	RV		RV+1L		FRC		FRC+1L		TLC	
	Posterior	**Remaining**	**Posterior**	**Remaining**	**Posterior**	**Remaining**	**Posterior**	**Remaining**	**Posterior**	**Remaining**
Volunteer	**slice**	**slices**	**slice**	**slices**	**slice**	**slices**	**slice**	**slices**	**slice**	**slices**
V1	14.95	11.75	21.38	12.11	23.9	12.19	21.13	10.72	17.45	10.3
V2	12.68	9.13	23.97	11.62	15.11	9.30	23.59	10.22	9.28	6.85
V3	8.28	11.15	18.18	8.58	5.59	9.06	10.16	8.65	7.64	7.40
V4	20.23	10.91	17.83	10.24	18.15	10.65	20.46	10.74	25.71	9.39
V5	9.98	10.98	27.03	11.03	5.37	9.42	9.53	9.60	8.29	8.25
V6	15.57	11.00	9.58	9.57	11.53	9.40	13.60	9.02	27.03	7.18

Table 6 Coefficient of variation (CoV) at each inflation level for metrics derived from hyperpolarized helium-3 (^{3}He) and xenon-129 (^{129}Xe)

^{3}**He**					^{129}**Xe**				
Acquisition	**TLV**	**VV**	**%VV**	**H_{score}**	**Acquisition**	**TLV**	**VV**	**%VV**	**H_{score}**
RV	3.40	3.05	1.29	5.32	**RV**	3.33	1.34	3.98	9.37
RV+1L	4.13	4.64	0.63	4.62	**RV+1L**	2.19	2.26	1.16	7.60
FRC	4.63	4.64	0.87	3.99	**FRC**	5.88	4.80	1.49	2.86
FRC+1L	3.42	3.42	0.38	2.74	**FRC+1L**	6.88	6.00	3.18	3.74
TLC	1.19	1.00	0.54	5.46	**TLC**	1.97	1.91	0.62	4.62

Table 7 Repeatability limit for percentage lung ventilated volume (%VV) and median value of the heterogeneity map (H_{score}) for images acquired using hyperpolarized helium-3 (^{3}He) and xenon-129 (^{129}Xe)

Acquisition	^{3}He %VV	^{3}He H_{score}	^{129}Xe %VV	^{129}Xe H_{score}
RV	5.08	1.80	11.69	3.72
RV+1L	2.19	1.86	3.06	2.62
FRC	2.90	1.29	4.50	1.07
FRC+1L	1.39	0.80	9.59	1.45
TLC	2.02	1.35	1.95	1.36

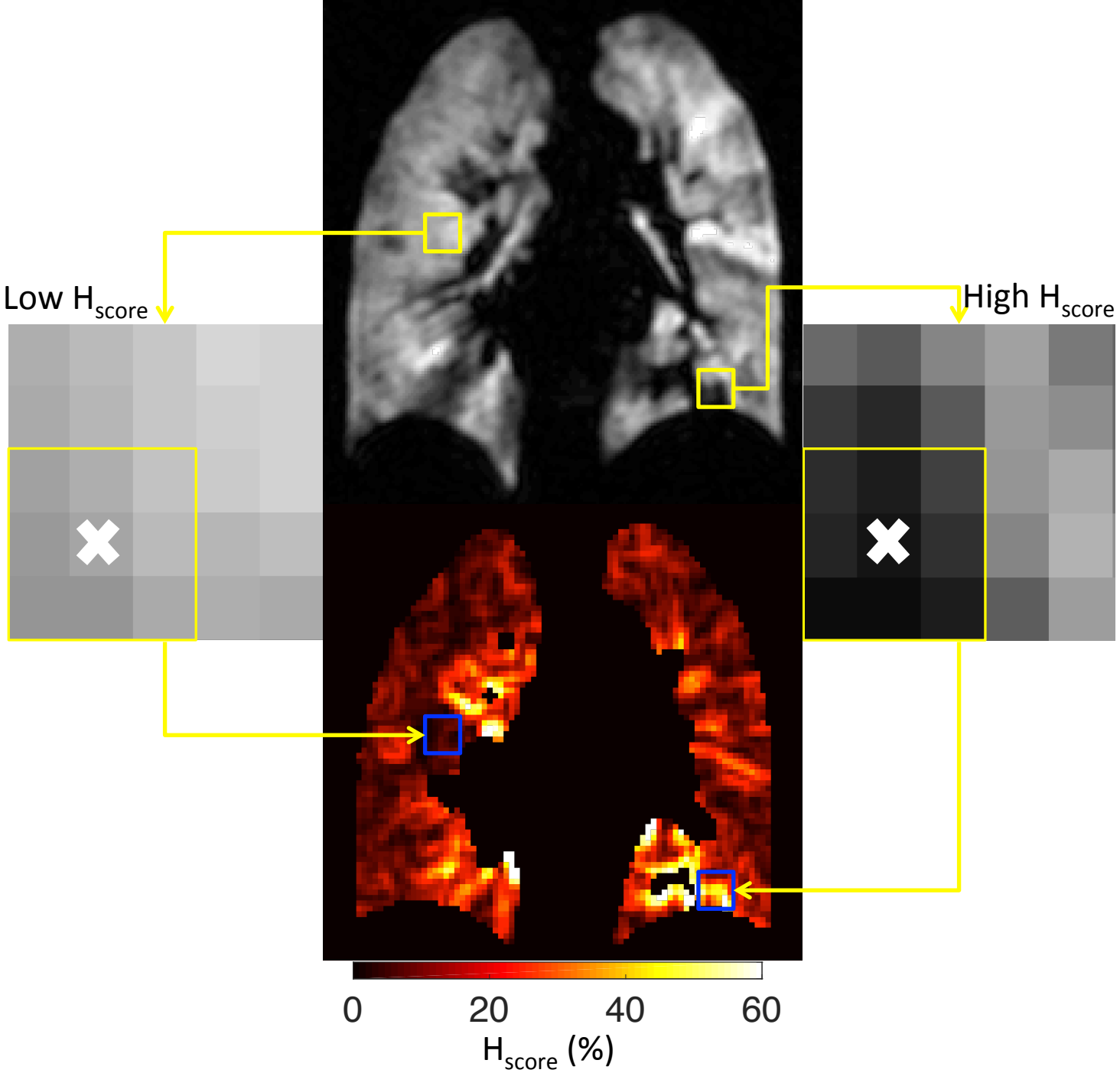
Low H_{score}
High H_{score}
0
20
40
60
H_{score} (%)

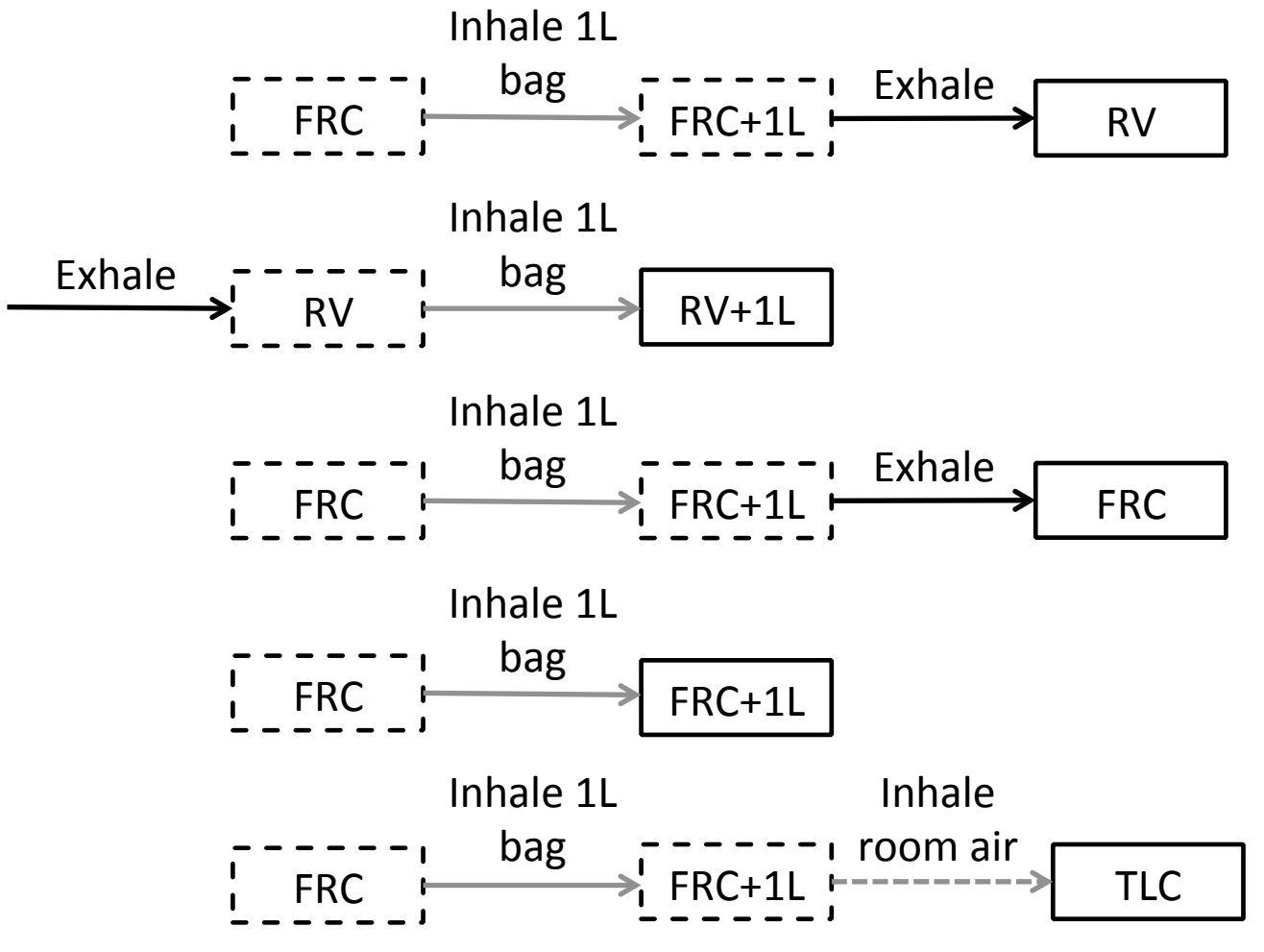
Inhale 1L
bag
FRC
FRC+1L
Exhale
RV
Inhale 1L
bag
Exhale
RV
RV+1L
Inhale 1L
bag
FRC
FRC+1L
Exhale
FRC
Inhale 1L
bag
FRC
FRC+1L
Inhale 1L
bag
Inhale
room air
FRC
FRC+1L
TLC

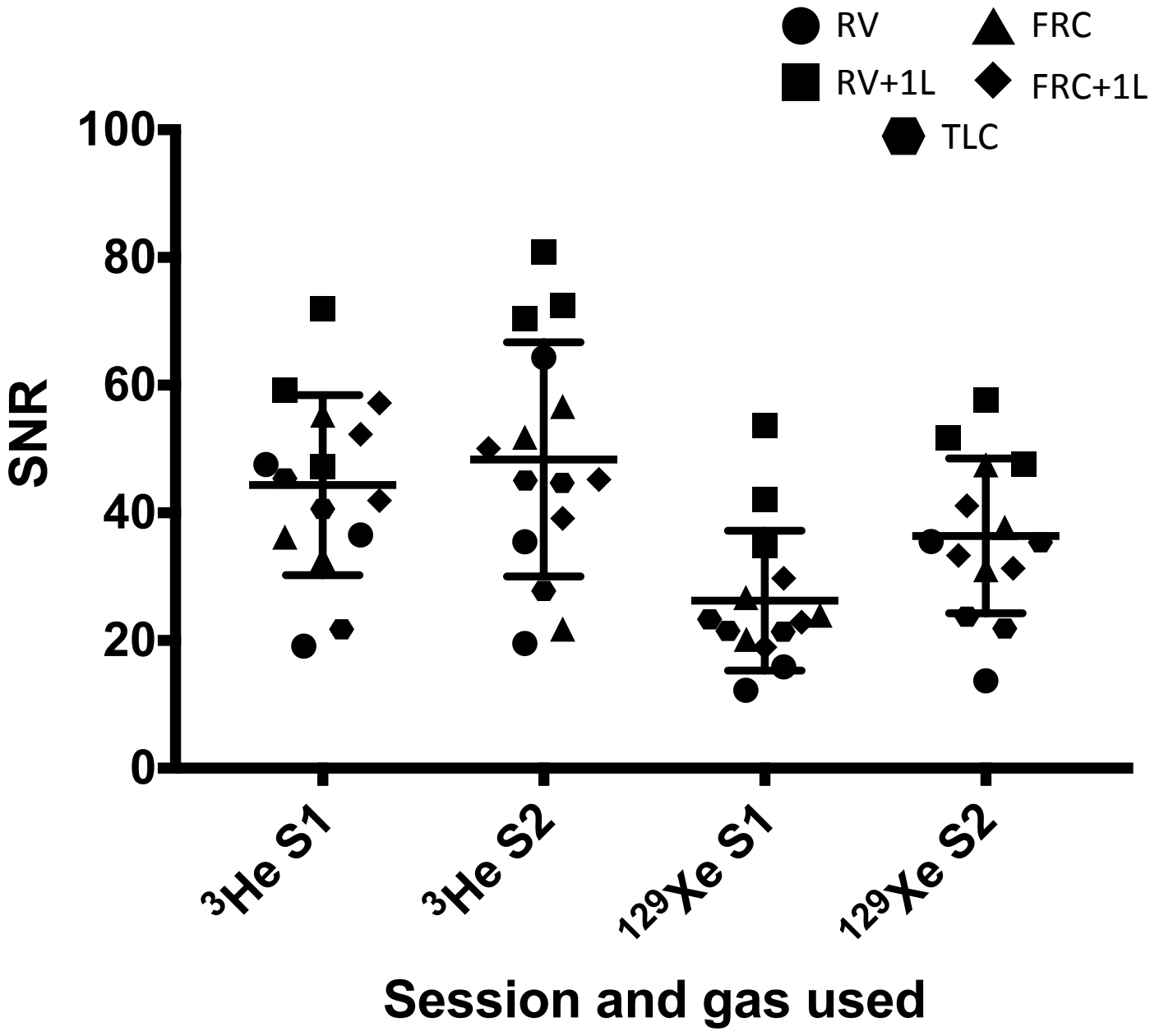
RV
FRC
RV+1L
FRC+1L
TLC
100
80
60
40
20
0
SNR
3He S1
3He S2
129Xe S1
129Xe S2
Session and gas used

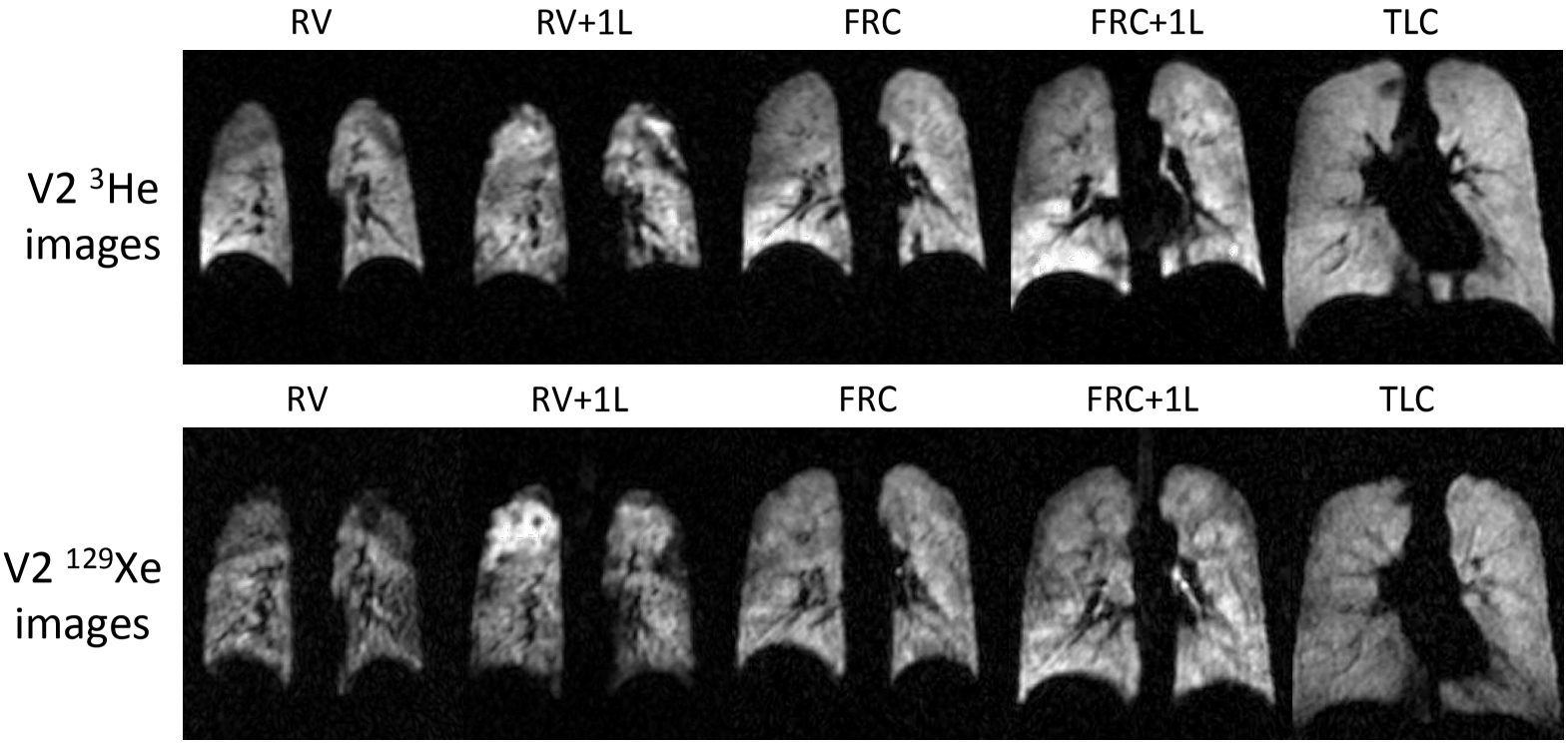
RV
RV+1L
FRC
FRC+1L
TLC
V2 ^{3}He images
RV
RV+1L
FRC
FRC+1L
TLC
V2 ^{129}Xe images

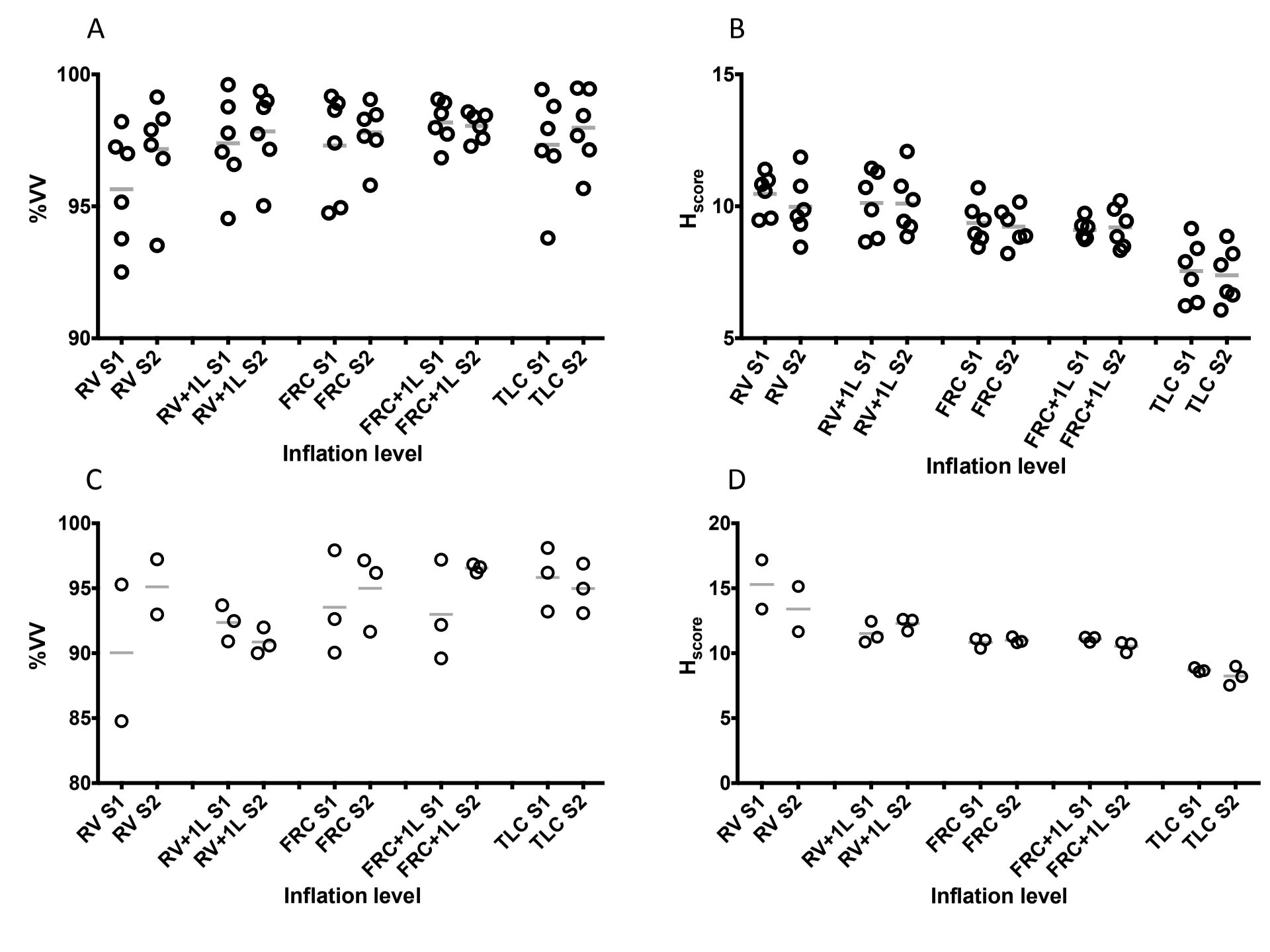
A
100
95
90
%VV
RV S1
RV S2
RV+1L S1
RV+1L S2
FRC S1
FRC S2
FRC+1L S1
FRC+1L S2
TLC S1
TLC S2
Inflation level
B
15
10
5
H score
RV S1
RV S2
RV+1L S1
RV+1L S2
FRC S1
FRC S2
FRC+1L S1
FRC+1L S2
TLC S1
TLC S2
Inflation level
C
100
95
90
85
80
%VV
RV S1
RV S2
RV+1L S1
RV+1L S2
FRC S1
FRC S2
FRC+1L S1
FRC+1L S2
TLC S1
TLC S2
Inflation level
D
20
15
10
5
0
H score
RV S1
RV S2
RV+1L S1
RV+1L S2
FRC S1
FRC S2
FRC+1L S1
FRC+1L S2
TLC S1
TLC S2
Inflation level

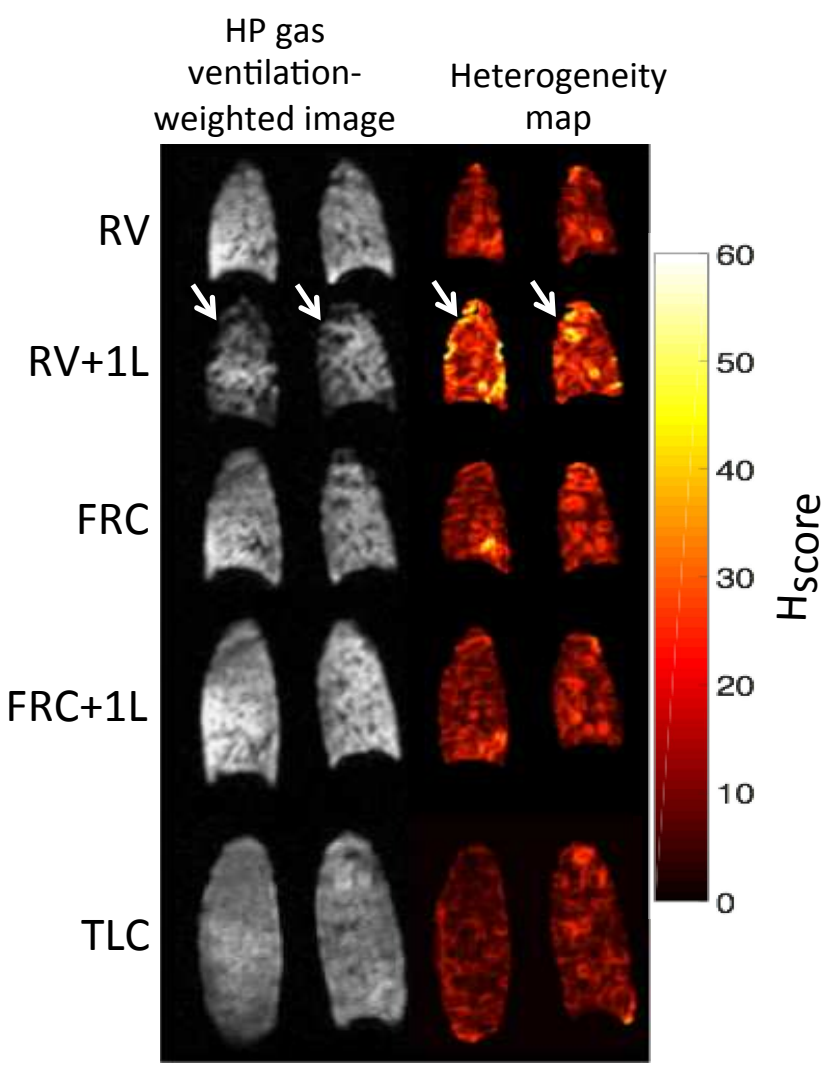
HP gas ventilation-weighted image
Heterogeneity map
RV
RV+1L
FRC
FRC+1L
TLC
60
50
40
30
20
10
0
Hscore

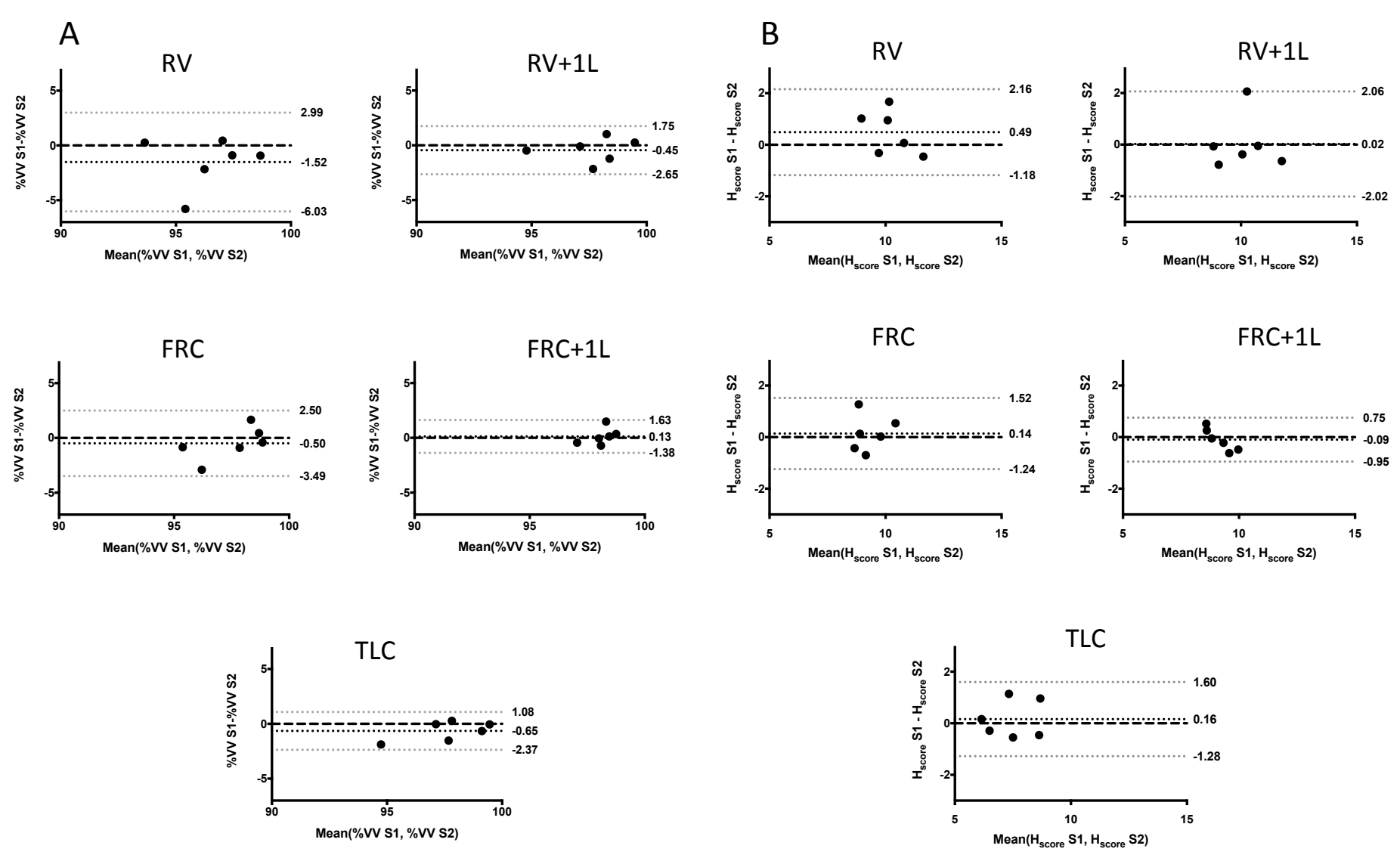
A
RV
%VV S1-%VV S2
2.99
-1.52
-6.03
Mean(%VV S1, %VV S2)
RV+1L
1.75
-0.45
-2.65
FRC
2.50
-0.50
-3.49
FRC+1L
1.63
0.13
-1.38
TLC
1.08
-0.65
-2.37
B
RV
Hscore S1 - Hscore S2
2.16
0.49
-1.18
Mean(Hscore S1, Hscore S2)
RV+1L
2.06
0.02
-2.02
FRC
1.52
0.14
-1.24
FRC+1L
0.75
-0.09
-0.95
TLC
1.60
0.16
-1.28

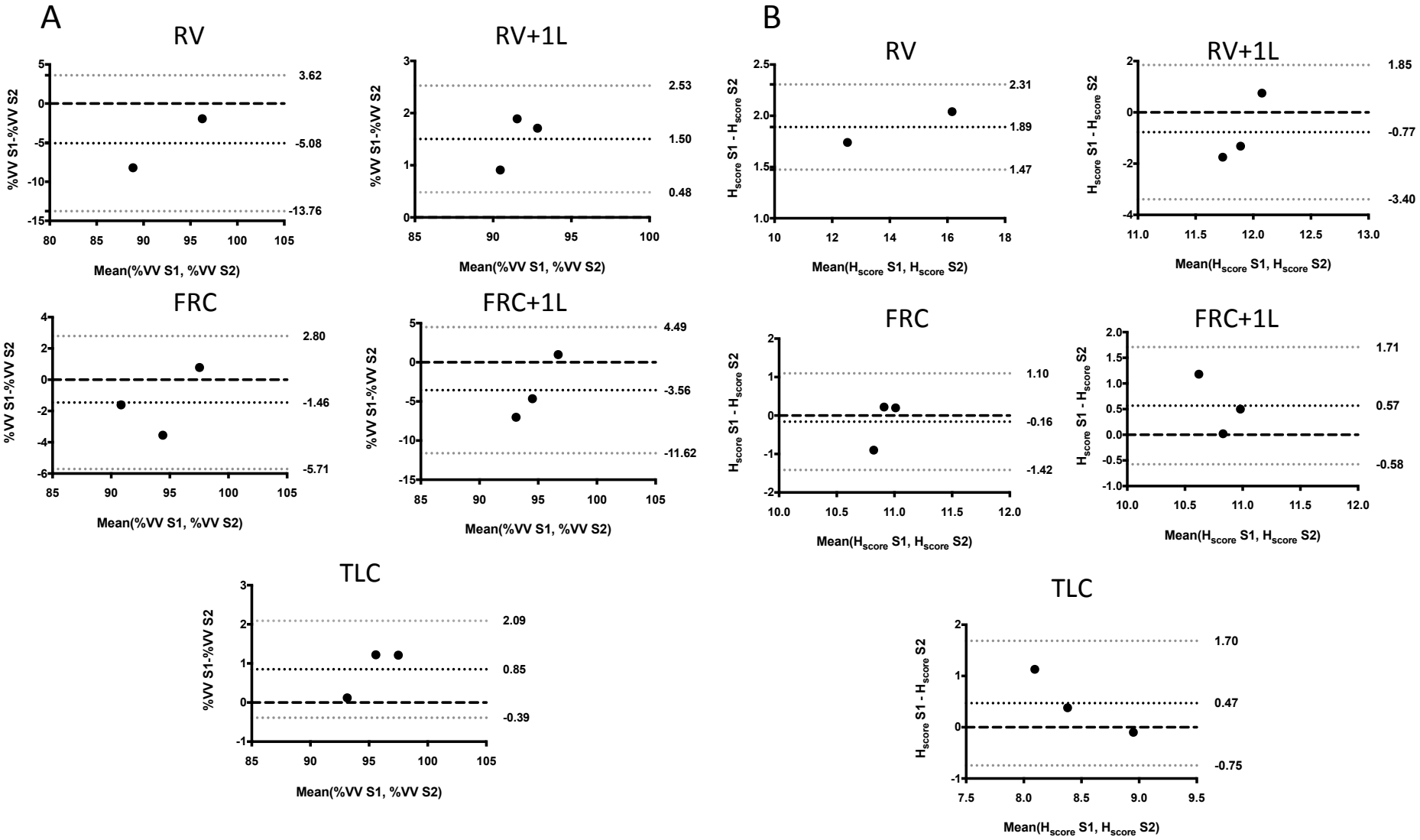
A
RV
%VV S1-%VV S2
Mean(%VV S1, %VV S2)
3.62
-5.08
-13.76
RV+1L
%VV S1-%VV S2
Mean(%VV S1, %VV S2)
2.53
1.50
0.48
FRC
%VV S1-%VV S2
Mean(%VV S1, %VV S2)
2.80
-1.46
-5.71
FRC+1L
%VV S1-%VV S2
Mean(%VV S1, %VV S2)
4.49
-3.56
-11.62
TLC
%VV S1-%VV S2
Mean(%VV S1, %VV S2)
2.09
0.85
-0.39
B
RV
Hscore S1 - Hscore S2
Mean(Hscore S1, Hscore S2)
2.31
1.89
1.47
RV+1L
Hscore S1 - Hscore S2
Mean(Hscore S1, Hscore S2)
1.85
-0.77
-3.40
FRC
Hscore S1 - Hscore S2
Mean(Hscore S1, Hscore S2)
1.10
-0.16
-1.42
FRC+1L
Hscore S1 - Hscore S2
Mean(Hscore S1, Hscore S2)
1.71
0.57
-0.58
TLC
Hscore S1 - Hscore S2
Mean(Hscore S1, Hscore S2)
1.70
0.47
-0.75

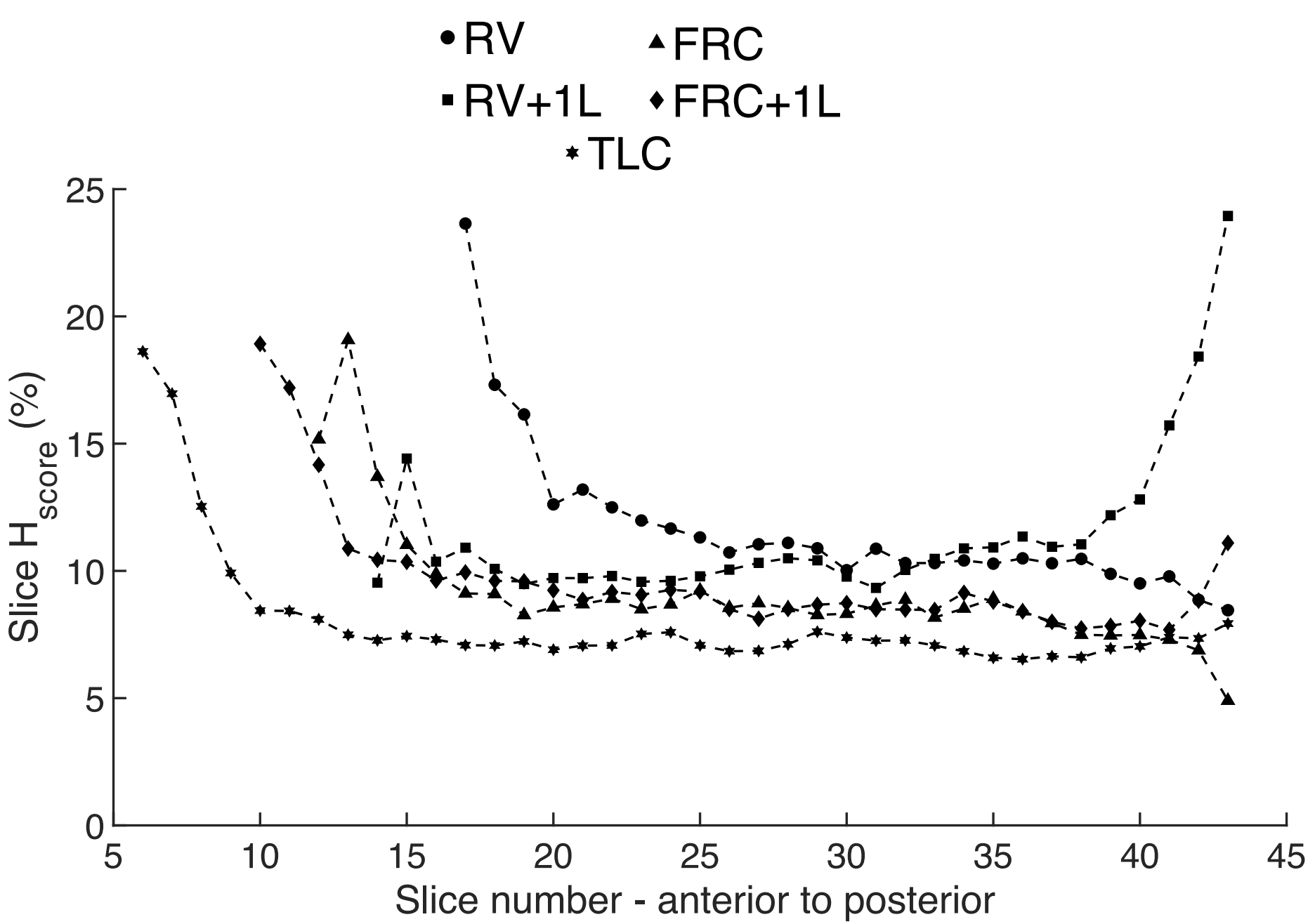
RV
FRC
RV+1L
FRC+1L
TLC
Slice H_{score} (%)
0
5
10
15
20
25
5
10
15
20
25
30
35
40
45
Slice number - anterior to posterior